

Cocrystal of Lutein with Improved Stability and Bioavailability

Chenxuan Zheng, Hao Wang, Ziyao Xiao, Zhixiong Sun, Junjie Bao, Wenjuan Dai, Qi Zhang,* and Xuefeng Mei*

Cite This: *ACS Omega* 2024, 9, 36389–36397

Read Online

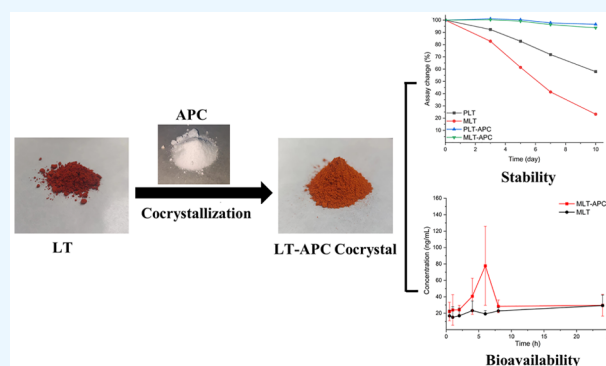
ACCESS |

Metrics & More

Article Recommendations

Supporting Information

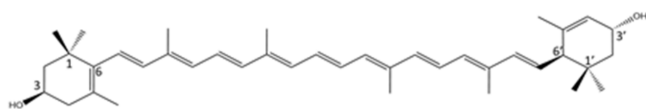
ABSTRACT: Lutein (LT) is a natural carotenoid and is widely used for its vision protection and antioxidant activity. However, the long-chain polyene structure makes lutein sensitive to light and oxygen and poses many difficulties in the production, processing, and storage. In addition, the special chemical structure of LT leads to low solubility and bioavailability. In this study, we propose an efficient solution to address these issues. A cocrystal of LT with adipic acid (LT-APC) was obtained for the first time. The cocrystals were fully characterized. After cocrystallization, the melting point of marketed LT was increased. The chemical stability of LT was significantly improved, and the influence of impurities on stability was limited. Dissolution experiments were performed in simulated gastric fluid (SGF) and simulated intestinal fluid (SIF) and the cocrystal generated a much higher apparent solubility. To deepen insight into the mechanisms underlying the cocrystal's improved solubility, wettability tests were performed by contact angle determination and film flotation methods. The cocrystal presented better wettability than the marketed LT. Finally, pharmacokinetic studies of marketed LT and its cocrystal were conducted in rats. The results showed that the cocrystal exhibited 3.4 times higher C_{max} and 2.2 times higher AUC at a single dose compared with marketed LT.



1. INTRODUCTION

Lutein (LT), and its stereo isomer zeaxanthin, are members of the xanthophyll family of carotenoids. It is a natural pigment mainly distributed in the petals of marigold flowers (Scheme 1). Its structure is consisted of two cyclohexene rings at both

Scheme 1. Chemical Structure of Lutein



ends and a long chain of polyenes in the middle.¹ Polyene chains give these molecules their characteristic color properties. Given their ability to absorb blue light, they have a yellow or orange appearance.² Hence, it is widely used as a colorant in feed and food additives.

LT is considered an important nutrient for the human body. LT and zeaxanthin are antioxidants that accumulate in the lens and retina of the human eye. They are hypothesized to play a role in humans similar to that in plants: to function as potent antioxidants and effective screeners of high energy blue light. Hence, LT is best known for its function in the protection and treatment of eye health.^{3,4} Naomichi Machida et al.⁵ determined the effects of lutein administration for 16 weeks on macular pigment optical density (MPOD), contrast sensitivity, and glare sensitivity. Compared with the placebo

group, the lutein group showed significantly improved MPOD, contrast sensitivity, and glare sensitivity at week 16 and significantly increased serum lutein levels at weeks 8 and 16. Supplementing with lutein can also improve cardiovascular function and protect skin.^{6,7} In vitro experiments with isolated neonatal rat cardiomyocytes (NRCMs) and cardiac fibroblasts (CFs) revealed that LT significantly attenuated Ang II-induced collagen expression in CFs, and cardiomyocyte hypertrophy. The Ang II-induced increases in superoxide generation, inflammation, and apoptosis in cultured CFs were strikingly prevented by LT. In vivo, LT was demonstrated to confer resistance to Ang II-induced cardiac remodeling in mice. A double-blinded, placebo-controlled, crossover study performed by S. GretherBeck, etc., demonstrated that LT could protect against solar radiation-induced skin damage by inhibiting UVA/B- and UVA1 radiation at a molecular level.

Nowadays, because of its unique properties, LT is widely used in feed, food, and nutraceuticals. However, poor stability has limited its use.^{8,9} Conjugated polyene chains cause LT to have poor chemical stability and it can easily lead to oxidative

Received: April 22, 2024

Revised: May 28, 2024

Accepted: May 30, 2024

Published: July 1, 2024



cleavage of polyene long chains under light and high temperature.¹⁰ This makes the storage and processing of luteins very difficult. During processing, foods are always required to be exposed to the high temperatures of cooking by boiling, sauteing, or steaming. In addition, LT is poorly absorbed and has low bioavailability for its lack of solubility in water.^{11–13} At present, chemical structure modification and physical embedding techniques are the main means to improve the stability and water solubility of lutein. Esterification is considered effective methods for improving the stability of lutein,^{14,15} due to the need for reabsorption after hydrolysis in the digestive tract,¹⁶ it is considered to be low bioavailability. Structural changes require reconsideration of safety implications. Encapsulation technology brings a high production cost. The drug packaging system is considered an effective solution to the stability problem of lutein,^{17,18} but still faces significant challenges in terms of component load, safety, and production cost control.

Recently, crystal technology was used to improve the stability of LT.¹⁹ Wei Guo et al. reported four crystal forms of LT: two anhydrous forms and two solvates. Stability tests of the four LT crystal forms showed that the LT solvates are more stable to UV radiation in comparison with solvent-free polymorphs. However, the solvates do not improve the stability of LT under heat irradiation. In addition, the solvates are unstable under high temperature condition. Above 50 °C, the solvates begin to lose their solvent and transform into solvent-free crystals. Such results indicate that, adding small molecular compounds may improve the stability of LT.

In this work, we successfully prepared a cocrystal of LT and adipic acid (APC) to improve the stability and bioavailability of LT. APC is a linear dicarboxylic acid, and it is naturally found in beets and sugar cane.²⁰ It is a nontoxic and biocompatible compound which has several applications in the food industry, e.g., as a flavorant, acidulating agent, and gelling aid.²¹ The cocrystal was fully characterized by powder X-ray diffraction (XRPD), Fourier transformation infrared (FTIR), differential scanning calorimetry (DSC) and thermogravimetric analysis (TGA). Stability tests of LT and its cocrystals under open, light irradiation, and simulated in-use conditions were performed. The dissolution rates of LT and the cocrystal were compared in SGF and SIF. Finally, the bioavailability of marketed LT (MLT) and its cocrystal was compared in rats.

2. MATERIALS AND METHODS

2.1. Materials. Lutein powder with a greater than 75% purity was purchased from Chenguang Technology Co., Ltd., Handan, China. Lutein standard was purchased from TMRM with a purity of 95.1%. APC, the other reagents, and all analytical grade solvents were purchased from Sinopharm Chemical Reagent Co., Ltd., Shanghai, China and used without further purification.

2.2. Purification. of LT. LT was purified by silica gel column chromatography (dichloromethane/methanol, v/v 100/1). The purity of the purified LT (PLT) was determined to be 94.9% using HPLC, and the zeaxanthin content was less than 3%.

2.3. Preparation of the LT-APC cocrystal. 10 g of PLT (16.7 mmol) and 2.57 g of APC (17.6 mmol) were mixed with 100 mL of acetone. The mixture was suspended at room temperature for 72 h in a container sheltered from light and protected by nitrogen. Filter yellow precipitate was dried in vacuum for 12 h to render the cocrystal PLT-APC as a yellow

powder. MLT without further purification also could be cocrystallized with APC to form the MLT-APC cocrystal. The preparation process is the same as that of the PLT.

To determine the stoichiometric ratio of LT and APC in the cocrystals, the amount of lutein in the cocrystals was determined using high performance liquid chromatography (HPLC), and the content of APC was determined by an automatic potentiometric titrator.

2.4. Powder X-ray Diffraction (PXRD). PXRD patterns were collected by using a Bruker D8 Advance X-ray diffractometer (Cu K α radiation). Voltage and current of the generator were set to 40 kV and 40 mA, respectively. Data over the range 3–40° 2 θ was collected with a scan rate of 5°/min at ambient temperature. Data were imaged and integrated with RINT Rapid and peak-analyzed with Jade 6.0 from Rigaku.

2.5. Differential Scanning Calorimetry (DSC). DSC experiments were performed on a TA Q2000 instrument under a nitrogen gas flow of 20 mL/min purge. A ground sample weighting 3–5 mg was heated in sealed nonhermetic aluminum pans at a heating rate of 10 °C/min and a cooling rate of 2 °C/min. Two-point calibration using indium and tin was carried out to check the temperature axis and heat flow of the equipment.

2.6. Thermogravimetric Analysis (TGA). Experiments for all of the samples were carried out on TGA-55 equipment (TA Instruments) with sample masses of approximately 10 mg. For all TGAs of the heating process, all the experiments began after weight stabilization. The powder sample was placed in an open aluminum oxide pan and heated to 410 °C at a heating rate of 10 °C/min. Dry nitrogen gas was used as the sample purge gas, with a flow rate of 60 mL/min.

2.7. FTIR Spectroscopy. FTIR spectra were collected by a Nicolet-Magna FT-IR 750 spectrometer in the range from 4000 to 350 cm⁻¹, with a resolution of 4 cm⁻¹ at ambient conditions.

2.8. Nuclear Magnetic Resonance (NMR) Spectroscopy. NMR experiments were conducted on a Bruker Avance III 600 Spectrometer operating at a frequency of 600 MHz. The measurements were performed at room temperature. The samples were dissolved in deuterated dimethyl sulfoxide (DMSO) as the solvent with a weight of approximately 10 mg.

2.9. Stability Tests. **2.9.1. Open Stability.** MLT, PLT, PLT-APC cocrystal, and MLT-APC cocrystal were stored at 40 °C, 75% RH under open condition without package and nitrogen protection, and the content of LT was measured on days 0, 3, 5, 7 and 10.

2.9.2. Photostability. To determine the photostability, MLT, PLT, PLT-APC cocrystal, and MLT-APC cocrystal were placed in a surface dish and placed in a strong light irradiation chamber, and the content of LT was measured at 0, 3, 5, 7, and 10 days. Turn the powder was turned once a day in the morning and night to ensure that the powder was evenly illuminated.

2.9.3. In-use Stability. To assess the in-use stability of MLT cocrystal in practical applications, a simplified capsule formulation was prepared by blending MLT-APC cocrystal powder with dextrin, silica, magnesium stearate, and other auxiliary materials, containing 20% LT. Four commercially available LT-containing products (Tablet A, Tablet B, Capsule A and Capsule B) fortified with other antioxidants were purchased from an e-commerce platform as references. The homemade LT capsules were packaged in white plastic vials, while the marketed samples were kept in their original

packaging. All analyses were carried out during the lifetime of each product. To evaluate the stability of the preparation in use, the product was stored at 25 °C and 60%RH, the package was opened once a day for sampling, and the content change of the product was measured on days 5, 10, 15, and 30.

2.10. Powder Dissolution Study. To evaluate the difference in the dissolution behavior of MLT and its cocrystals in practical applications, powder dissolution experiments of MLT and MLT-ACP cocrystals are carried out in simulated gastric Fluid (SGF) and simulated intestinal Fluid (SIF) with 0.1% sodium dodecyl sulfate (SDS). SIF was prepared by dissolving 6.8 g of KH₂PO₄ in 500 mL of water and then adjusting the pH to 6.8 with a 0.1 mol/L NaOH solution. SGF was obtained by mixing 16.4 mL of 10% HCl solution and 800 mL of water and finally diluted to 1000 mL with water. Dissolution experiments were performed at 37 °C using a Mini-Bath dissolution device equipped with a Julabo ED-5 heater/cycler. Twenty mg of test samples were added to 15 mL of the mock digest. The stirring speed was set to 100 rpm. Both the cocrystals and the raw materials passed through a 100-mesh screen to minimize the effect of particle size on the dissolution results. Samples were collected at 5, 10, 20, 40, 60, 90, and 120 min each time and filtered through a 0.22 μm nylon filter. 0.5 mL of the filtrate was extracted with a 0.5 mL mixed solution (70% *n*-hexane (Hex) + 30% ethyl acetate (EA)) containing 0.3% VE, sonicated for 5 min, centrifuged at 14000 rpm for 5 min, then the water later was removed, and the organic layer was collected for determination of LT concentration by HPLC.

2.11. Contact Angle Measurements. Water contact angles of LT and LT-APC were measured using a contact Angle device from OCA20, Dataphysics Co., Ltd., Germany. Before the test, samples were pressed into sheets and placed on glass plates. The contact angles are measured by the sessile drop method with pure water.

2.12. Wettability Test. The wettability test was performed in SGF and SGF with 0.1% sodium dodecyl sulfonate (SDS) or tween 80 using film flotation methods. A total of 5 mg of MLT and MLT-APC powders were put on the solution (the powder was passed through a 180-mesh screen before the experiment), and the wettability was compared by calculating the powder sinking speed.

2.13. Pharmacokinetic (PK) Study. PK experiments were conducted using a self-controlled design. The samples were evenly dispersed in a flour-oil suspension (30% olive oil, 70% flour suspension (0.3 g of flour was suspended in 1 mL of water)). Six male Sprague–Dawley rats, weighing 300–320 g were used in each group. The interval between each dose was 1 week, and the next set of experiments was performed after LT metabolism was complete. Each was administered by gavage at a dose of 50 mg/kg (expressed as LT equivalent). At the end of the administration, approximately 400 μL of blood samples were taken from each rat from the orbital sinus at 30, 60, 120, 240, 360, 480, and 1440 min and placed into heparinized tubes. 100 μL of plasma was removed, 100 μL of methanol was added, vortex oscillated for one min, then 400 μL of Hex was added, vortex oscillated for one min, centrifuged at 14000 rpm for 5 min. The supernatant was removed to 96-well plate, dried with nitrogen gas, and 200 μL of methanol was added, shaken for 10 min, centrifuged for 5 min, and then the sample was analyzed by HPLC. Plasma was processed immediately after removal; sample processing and analysis were performed under dark light conditions.

2.14. HPLC Analysis. An Agilent 1260 series HPLC instrument was used to determine the content of LT. HPLC was performed using a four-element pump (G1311C), diode array detector (G1315D), and ZORBAX RX-SIL column, 4.6 × 250 mm, 5-Micron. Detector set to 446 nm. The mobile phase consisted of Hex and EA (60/40, v/v) and was run for 20 min at 1.5 mL/min. The sample size was 10 μL, the column temperature was 25 °C, and a mixed solvent (EA/Hex, 30/70, v/v) containing 0.3% VE was used as the extraction solvent and injection solvent.

2.15. Bioanalytical Method. The amount of lutein in plasma was analyzed using the same HPLC instrument as in 2.14. Chromatography consisted of a Column NO. ZORBAX ECLIPSE Plus C18 (50 × 4.6 mm, 1.8 μm). The mobile phase consisted of water and acetonitrile (2/98, v/v) at a flow rate of 1.5 mL/min. An injection of 40 μL was performed, and the column temperature was set to 25 °C. The detector was set at 446 nm.

2.16. Potentiometric Titration. The content of ACP was determined using an 809 Titrand automatic potentiometric titrator from Metrohm Co., Ltd., Herisan, Switzerland. 60 mg of ACP was weighted and dissolved in 60 mL methanol and titrated with 0.1 mol/L sodium hydroxide aqueous solution.

3. RESULTS AND DISCUSSION

3.1. PXRD Analysis and Stoichiometric Ratio Determination. In the screening process, PXRD analysis is a

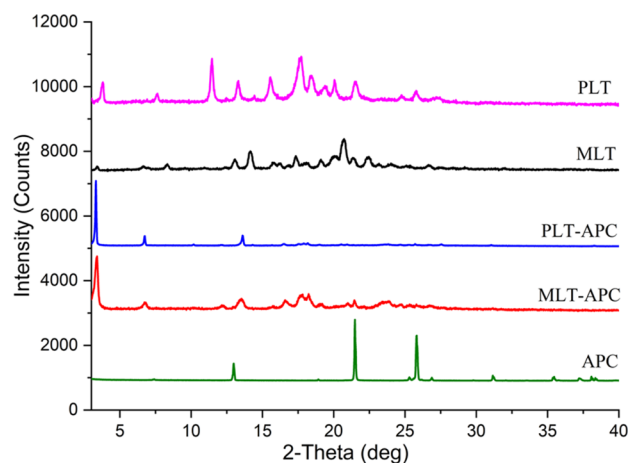


Figure 1. Compared PXRD patterns of LT and its cocrystals.

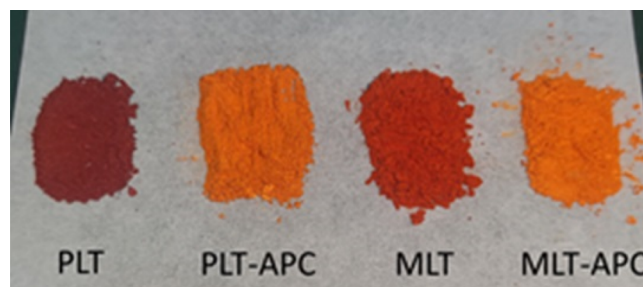
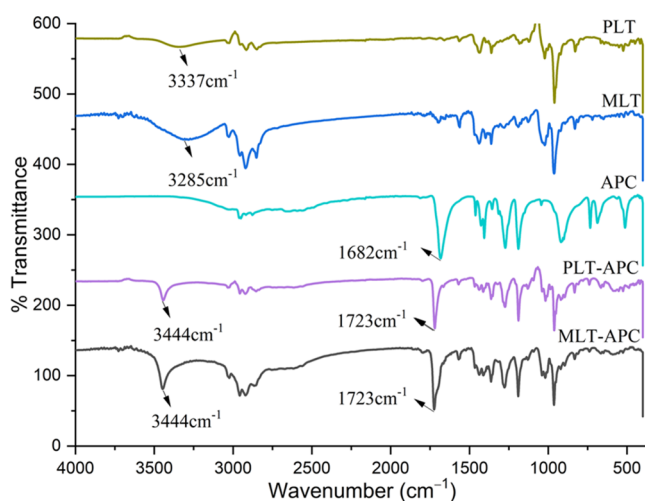


Figure 2. Bulk powders of PLT, MLT, PLT-APC, and MLT-APC.

primary method to detect the formation of new multi-component phases and determine the purity of new solid substances. Four polymorphs of LT were reported¹⁹ and the PLT we used in this paper is polymorph I. The PXRD patterns

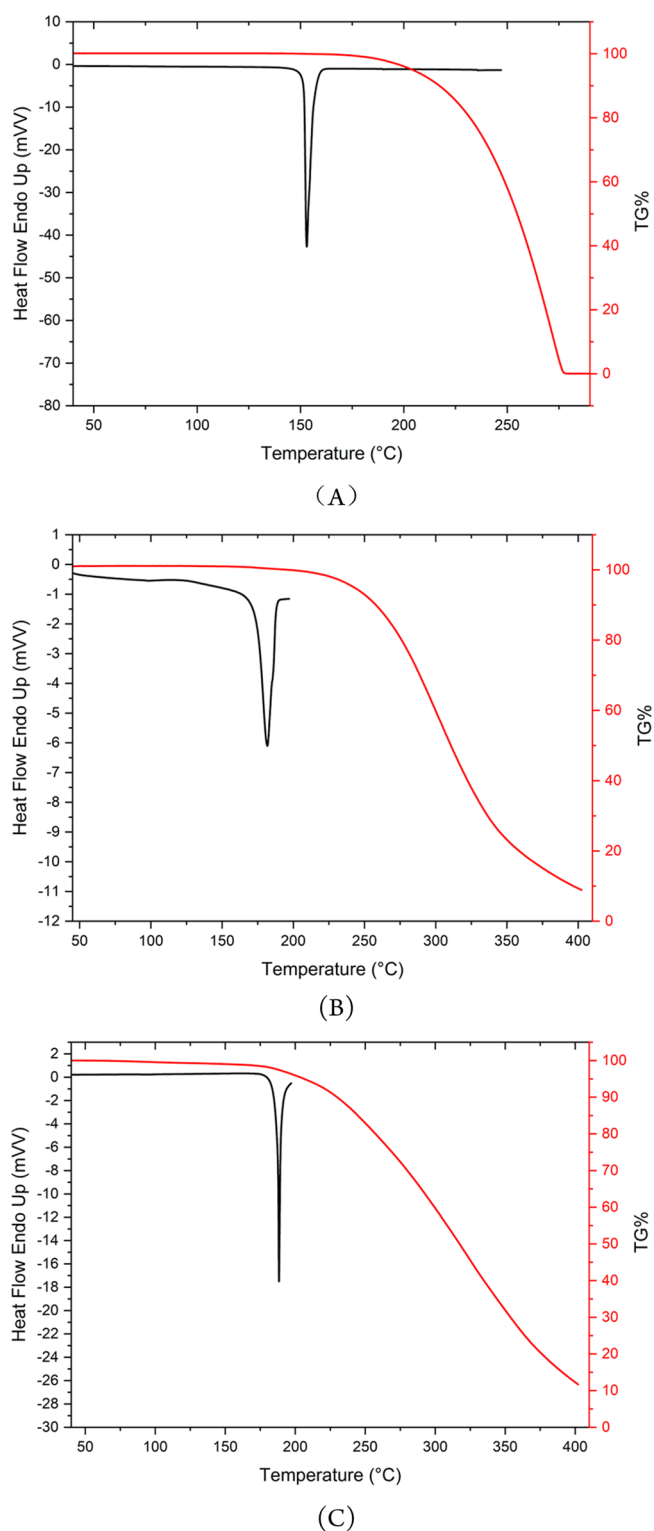
Table 1. LT and APC Contents in the LT Powder Samples

	LT%	APC%	LT: APC
PLT	94.9	-	-
MLT	78.2	-	-
PLT-APC	75.4	19.7	0.98:1
MLT-APC	68.0	18.5	0.94:1

**Figure 3.** Compared IR spectra of lutein and the cocrystal.

of LT different polymorphs and its cocrystals are presented in Figure 1 and Figure S1. APC has characteristic peaks at 2θ 3.78°, 7.61°, and 11.44°. PLT and MLT spectra exhibit different PXRD plots. They both have peaks at 2θ 3.8°, 13.3°, 14.4°, 17.7°, and 18.4°. However, PLT shows characteristic peaks at 2θ 7.6°, 11.46°, and MLT presents new peaks at 2θ 8.5°, 6.8°. Such differences may be due to the impurities in the marketed raw materials. PLT-APC cocrystal and MLT-APC cocrystal exhibit very similar PXRD patterns. They show significantly different curves from that of PLT and MLT. They both have new characteristic peaks at 2θ 3.36°, 6.75°, 13.53°, and 16.56°. Such PXRD differences confirm the creation of new phases. The similar PXRD patterns of PLT-APC and MLT-APC indicate that the impurity does not affect the formation of cocrystals. In addition, the cocrystal formation can also be confirmed by the color change among the cocrystallization process (Figure 2). After cocrystallization, the color of PLT was changed from deep red to orange and the color of MLT was changed from red to orange.

The cocrystal was prepared by slurring more than 10 times, and the obtained cocrystals present similar properties. Such results confirmed that the resulting cocrystals had a similar composition. The stoichiometric ratios of LT and APC in LT-APC cocrystal synthesized by suspension method were determined by content comparison and ^1H NMR. LT content was determined by HPLC and APC content was checked by potentiometric titrator, respectively. In the PLT-APC, the content of lutein is about 75.4%, the content of adipic acid is about 19.7%; in the MLT-APC, the content of lutein is about 68.0%, the content of adipic acid is about 18.5%. The calculated stoichiometric ratios are shown in Table 1, and the calculation process is placed in the Supporting Information. Such results indicate that the stoichiometric ratios of LT and APC in the cocrystals are about 1:1. The stoichiometric ratio was also verified using ^1H NMR. In the ^1H NMR spectra (Figures S1 and S2) of PLT-APC cocrystal, the peak areas

**Figure 4.** Compared DSC-TG curves of LT and its cocrystal: (A) APC, (B) PLT, and (C) PLT-APC.

(normalized) corresponding to the hydrogen atoms connected to the 3, and 3' carbon atoms on the hexatomic rings at δ 4.05 and δ 3.75 are 0.95 and 1.01, respectively, with each peak representing one hydrogen atom. The peak areas at δ 2.21 and δ 1.50 corresponding to the hydrogen atom on methylene of APC were 4.24 and 3.95, respectively, with each peak

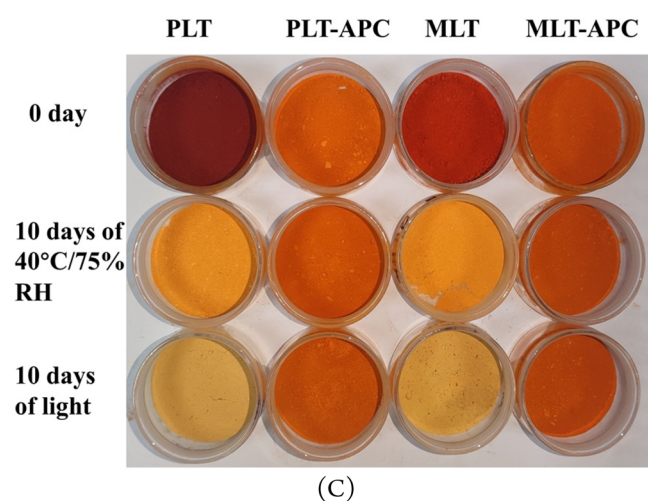
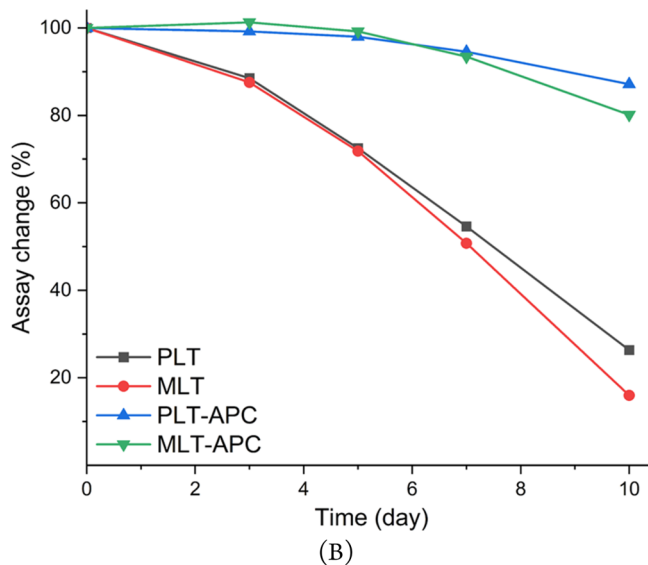
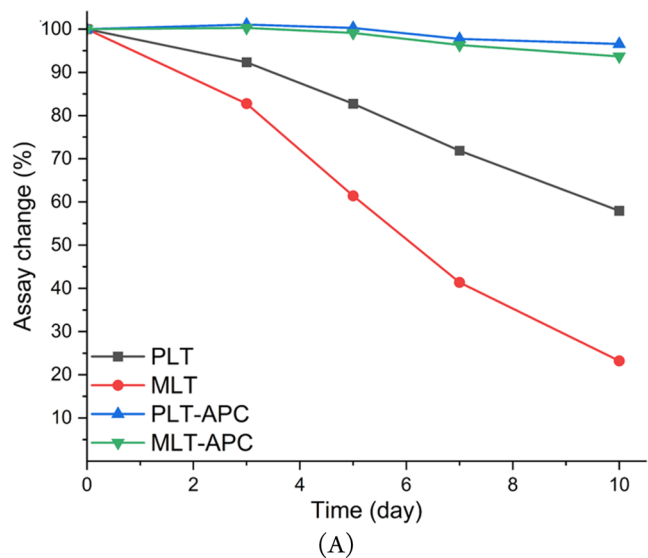


Figure 5. Stability results (the content of lutein at day 0 was set as 100%): (A) assay changes at 40 °C/75RH open condition, (B) assay changes under strong light irradiation conditions, and (C) color changes among the stability experiments.

representing four hydrogen atoms. The results confirmed the 1:1 stoichiometric ratio of LT to APC in the cocrystal.

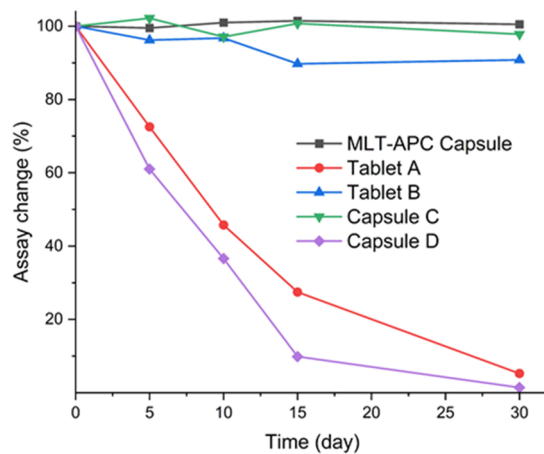


Figure 6. Assay changes of lutein in-use stability studies (the content of LT at day 0 was set as 100).

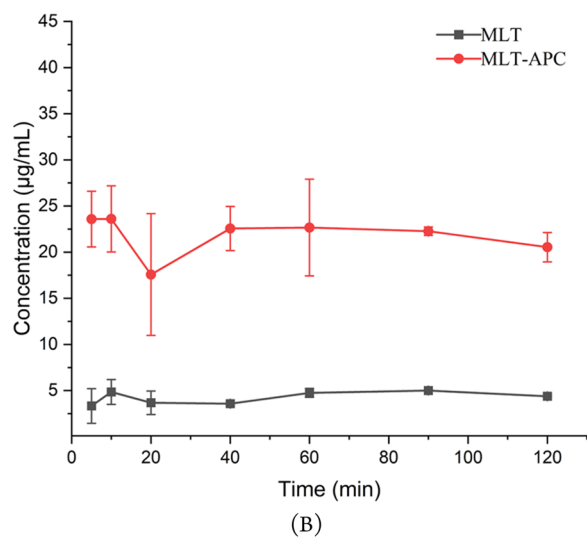
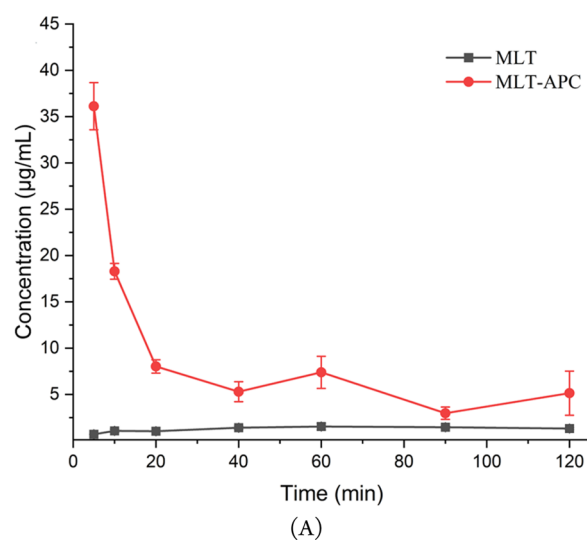


Figure 7. Compared dissolution profiles for MLT and MLT-APC: (A) in SGF and (B) in SIF.

3.2. FTIR Spectra. The FTIR spectra of LT, APC, and the cocrystals are shown in Figure 3. PLT-APC and MLT-APC present very similar FTIR curves. They both exhibit significantly different FTIR spectra from those of LT and



Figure 8. Contact angle images of MLT and MLT-APC.

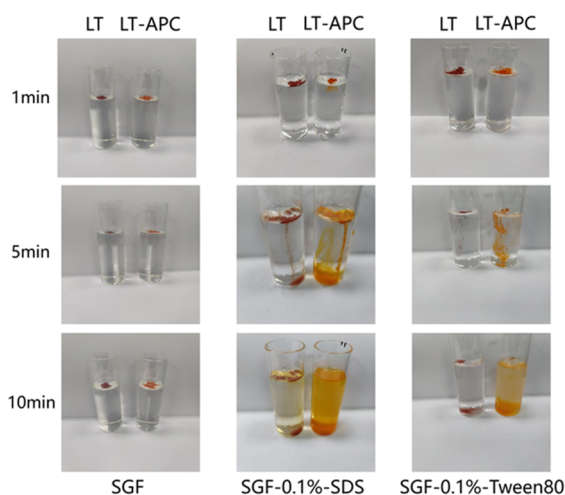


Figure 9. Results of the film flotation experiments.

APC. In the FTIR spectra of LT (both PLT and MLT), there is a wide peak at $3111\text{--}3561\text{ cm}^{-1}$, corresponding to the stretching of unassociated O–H in the LT molecule. In comparison, in the FTIR spectra of both PLT-APC and MLT-APC, there are sharp peaks at 3444 cm^{-1} , representing the stretching of the associated O–H in the cocrystals. Such changes indicate the formation of strong hydrogen-bond interaction on the hydroxyl group of the LT molecules in the cocrystals. In the FTIR spectrum of APC, there is a spike at 1682 cm^{-1} , indicating the C=O stretching vibration in the APC molecule. In the FTIR spectra of the cocrystals, the peak corresponding to the C=O stretching vibration is blue-shifted from 1682 to 1723 cm^{-1} . The blue shift also indicates the strong hydrogen bond interaction between LT and APC in the cocrystals.

3.3. DSC and TGA Analysis. The DSC and TGA curves of APC, PLT, MLT, PLT-APC, and MLT-APC are shown in Figure 4 and Figure S4. Their thermodynamic parameters (fusion enthalpies, onset temperatures, and peak temperatures) were presented in Table S1. TGA analysis showed that the weight did not change before the PLT-APC and MLT-APC solid melted, indicating that the cocrystals did not contain solvent. APC presents a sharp peak at $153.0\text{ }^{\circ}\text{C}$ corresponding to its melting. PLT and MLT show sharp melting peaks at temperatures of 182.0 and $168.8\text{ }^{\circ}\text{C}$ (Table S1), respectively.

Table 2. Pharmacokinetic Parameters of the PK Experiments

	T_{\max} (h)	C_{\max} (ng/mL)	$AUC_{0\text{--}8\text{h}}$ (h ng/mL)	$T_{1/2}$ (h)	CL/F(L/(h kg))	MRT (h)
LT	4	23.2 ± 11.6	148.6 ± 24.7	63.7 ± 12.5	49.1 ± 24.8	13.3 ± 2.2
LT-APC	6	77.8 ± 48.2^a	325.0 ± 146.8^a	37.3 ± 30.9	32.9 ± 18.2	11.5 ± 1.1

^aSignificant difference between LT-APC and LT at the 0.05 level (P values for C_{\max} and AUC are 0.039 and 0.029, respectively).

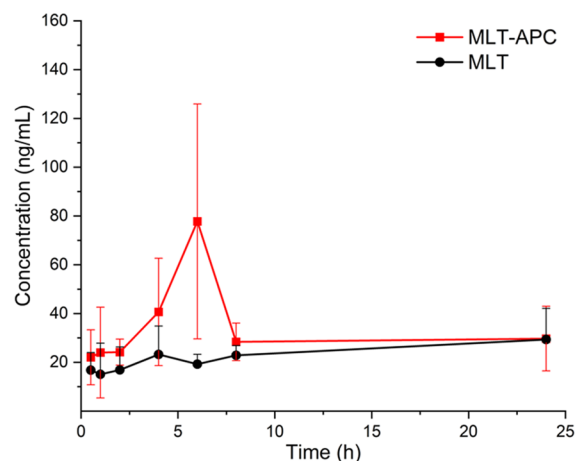


Figure 10. Plasma concentration–time curves of MLT-APC cocrystal and MLT (data are expressed as mean \pm SD, $n = 6$).

The high purity LT has a much higher melting point. However, the cocrystals prepared with PLT and MLT have a similar melting point. PLT-APC and MLT-APC show sharp melting peaks at temperatures of 188.0 and $187.8\text{ }^{\circ}\text{C}$, respectively (Figure S3, Table S1). Co-crystallization inhibits the influence of impurities on the melting point and may lower the influence of impurities on the stability.

3.4. Stability Studies. **3.4.1. Open Stability.** The open stability of PLT, MLT, PLT-APC, and MLT-APC was investigated at $40\text{ }^{\circ}\text{C}$ and 75% RH under open conditions without package and nitrogen protection. The results (Figure 5A) show that, after 10 days, the LT content in PLT and commercially available raw materials MLT was decreased to 58.0% and 23.2%, respectively. In contrast, the LT content in PLT-APC and MLT-APC decreased only to 96.6% and 93.7%, respectively. Under harsh conditions without deliberate antioxidant protection, LT was destroyed rapidly and the cocrystals exhibit excellent stability. In addition, high purity LT have much better stability than low purity LT. Impurities may cause a decrease in the stability of LT. In comparison, the cocrystal prepared with low purity LT (MLT-APC) presents similar stability to that of the cocrystal prepared with high purity LT (PLT-APC). Co-crystallization inhibits the influence of impurities on the stability.

3.4.2. Photo Stability. Furthermore, the photo stability of LT and its cocrystals under intense light irradiation was also tested. PLT, MLT, PLT-APC, and MLT-APC were placed in a strong light stabilization box, and the samples were turned twice daily for uniform exposure to light. Samples were collected at different time intervals for measurement of LT content on days 0, 3, 5, 7, and 10. The results (Figure 5B) present that after intense light irradiation for 10 days, the content of LT in PLT and MLT decreased to 26.3% and 16.0%, respectively. In comparison, the content of LT in PLT-APC and MLT-APC cocrystals was only decreased to 87.1%

and 80.1%, respectively. Such results indicate that compared to LT itself, the cocrystals also exhibit much better photostability.

The color changes among the stability studies also confirm the improved stability of the cocrystals. As shown in Figure 5C, after 10 days, under high temperature and light conditions, the color of the cocrystals remain unchanged. In contrast, the color of PLT was changed from deep red to light yellow, and the color of MLT was changed from red to light yellow.

3.4.3. In-Use Stability. For convenience purposes, multidose packaging is utilized for health food products, which require multiple openings and resealing during use. Considering compliance factors, it is important to ensure that the product remains stable, even after being opened for several weeks or longer periods of time. In-use stability testing aims to provide information for the labeling on the preparation, storage condition, and utilization period of multi dose products after opening. The test should be designed to simulate the use of the finished pharmaceutical product in practice, taking into consideration the filling volume of the container. LT is an extremely sensitive substance to both heat and oxygen. Hence, investigating the in-use stability of LT becomes necessary.

To test its in-use stability, MLT-APC was made into capsules by blending the MLT-APC cocrystal powder with dextrin, silica, and other auxiliary materials. In the stability experiments, four marketed LT samples (two tablets and two capsules, set as Tablet A, Tablet B, Capsule C, and Capsule D) and homemade capsules were stored at 25 °C, 60% RH and the packages were opened once a day. The results are presented in Figure 6. After 30 days, obvious degradation was observed in the two marketed LT products (Tablet A and Capsule D). The assay results of LT in these samples were lowered to 5.3% and 0.84%, respectively. Less degradation was observed in the other two marketed LT products (Tablets B and Capsule C). The assay of LT in these samples were dropped to 90.8% and 97.8%, respectively. In comparison, no obvious change in LT content was observed in the cocrystal capsule. MLT-APC cocrystal significantly improved the in-use stability of LT and ensured the safety and efficacy in daily use of LT.

3.5. Powder Dissolution. Dissolution studies of MLT and its cocrystal MLT-APC were performed in SGF and SIF with 0.1% SDS. The results are shown in Figure 7. A “rapid parachute” phenomenon of MLT-APC in SGF appeared. The content of LT reached a maximum of 36.1 $\mu\text{g}/\text{mL}$ at the fifth minute, which was 51.6 times higher than that of MLT. The concentration of LT gradually decreased and reached equilibrium after 40 min. After the dissolution experiments, residual sample was checked by PXRD (Figure 5SC) and the cocrystal was kept unchanged. Such a result indicates that the drop in concentration is not due to the phase transition. Considering the instability of LT, the decrease in the concentration may be due to the decomposition of LT in an acidic environment. In SIF, the content of LT reached maximum for MLT-APC and MLT both at the 10th minute (23.6 $\mu\text{g}/\text{mL}$ for MLT-APC and 4.9 $\mu\text{g}/\text{mL}$ for MLT). MLT-APC presented a 4.9 times higher apparent solubility than that of MLT. In SIF, MLT and MLT-APC both reached equilibrium quickly, and the concentration of LT could remain unchanged for a long time. The residues after dissolution experiments were checked by PXRD (Figure 5S). The results showed that after the dissolution experiments MLT and MLT-APC both remain unchanged.

3.6. Wettability Test. According to Yalkowsky and Valvani,²² the aqueous solubility, X_a , is generally defined as $\log X_a = \log X_i - \log \gamma$. X_i is the ideal solubility, and γ is the activity coefficient of the solute in water. X_i could be mathematically expressed as $\log X_i = -0.01(T_m - 25)$, where T_m represents the melting point of solute in Celsius. Higher melting points may lead to lower X_i , reducing the solubility. In this work, the cocrystals have similar or higher melting points, indicating that the ideal solubility X_i is not the key factor for the solubility enhancement. Hence, the enhanced dissolution behavior of the cocrystal should result from the decreased activity coefficient γ . The activity coefficient represents the decrease in aqueous solubility due to intermolecular interaction differences between solute and solvent molecules. The introduction of APC can increase the intermolecular interaction between the solute and water (S–W interaction) and then improve the solubility. The increased S–W interaction could be verified by wettability tests. Better wettability represents higher S–W interaction.²³ Wettability tests were performed by contact angle determining and film flotation methods. MLT and MLT-APC water contact angle was measured by sessile drop goniometric method with pure water and the images of the contact angle of water drop placed on MLT and MLT-APC are presented in Figure 8. The water contact angles of MLT and MLT-APC are $100.37 \pm 0.97^\circ$ ($>90^\circ$) and $85.32 \pm 0.85^\circ$ ($<90^\circ$), respectively. Cocrystal exhibits a better wettability than that of MLT. Film flotation experiments were conducted in SGF with/without surfactants. The results are shown in Figure 9. In pure SGF, neither MLT nor MLT-APC could sink into the solution. Surfactants significantly improved the wettability of MLT and MLT-APC. In SGF containing 0.1% SDS or tween 80, the MLT-APC powder sank into the solution much faster than that of MLT. Such results also confirmed the better wettability of the cocrystal. The improved wettability may finally result in solubility and dissolution enhancement of the cocrystal.

3.7. PK Study. In vivo PK studies of MLT-APC cocrystals and MLT raw materials were performed on the same batch of fasted male rats. The pharmacokinetic parameters are shown in Table 2 and the mean plasma concentrations of LT relative to the time distribution is shown in Figure 10. The results show that the cocrystal had a much higher in vivo bioavailability than that of the marketed MLT. The C_{max} values of cocrystal and commercially available MLT were 77.8 and 23.2 ng/mL, respectively. The maximum LT concentration produced by this cocrystal was 3.4 times higher than that of the MLT. The AUC 0–8 h for MLT-APC and MLT were 325.0 h ng/mL and 148.6 h ng/mL, respectively. The first 8 h of cocrystals yielded a 2.2 times larger AUC than that of the commercially available MLT. PK studies have shown that the cocrystal of lutein can indeed enhance its oral absorption by increasing its solubility and dissolution rate.

4. CONCLUSION

In summary, we have prepared a new cocrystal of LT for the first time. The cocrystals were fully characterized by PXRD, FTIR, DSC, and TGA. Purified PLT has a melting point much higher than that of the marketed low purity MLT. However, the cocrystals prepared with PLT and MLT presented similar melting points. Open, photo, and in-use stability of LT and its cocrystals were tested. PLT had a much better open stability than that of MCT. PLT-APC and MLT-APC cocrystals exhibited similar and significantly improved stability. Co-

crystallization limited the influence of the impurity on the stability. Cocrystals also obviously improved the photo and in-use stability. Dissolution experiments of MLT and its cocrystal were performed in SIF and SGF. In SGF, the cocrystal showed a “rapid parachute” phenomenon and presented 51.6 times higher C_{max} than that of MLT. In SIF, MLT and the cocrystal reached equilibrium quickly and the cocrystal had a 4.9 times higher apparent solubility than that of MLT. To deepen insight into the mechanisms underlying the cocrystal’s improved solubility, wettability tests were performed by contact angle determination and film flotation methods. The cocrystal presented better wettability than that of MLT. Finally, pharmacokinetic studies of MLT and its cocrystal were conducted in rats. The results showed that, the cocrystal exhibited 3.4 times higher C_{max} and 2.2 times higher AUC at a single dose compared with marketed MLT.

■ ASSOCIATED CONTENT

SI Supporting Information

The Supporting Information is available free of charge at <https://pubs.acs.org/doi/10.1021/acsomega.4c03864>.

Stoichiometric ratios calculation, Figure S1: ^1H NMR spectra of purified lutein; Figure S2: ^1H NMR spectra of PLT-APC cocrystal; Figure S3: DSC-TG pattern of MLT (a) and MLT-APC (b); Table S1: thermodynamic parameters of PLT and PLT-APC; Figure S4: PXRD patterns for MLT and MLT-APC before and after dissolution test (PDF)

■ AUTHOR INFORMATION

Corresponding Authors

Qi Zhang – Pharmaceutical Analytical&Solid-State Chemistry ResearchCenter, Shanghai Institute of Materia Medica, ChineseAcademy of Sciences, Shanghai 201203, People’s Republic of China; orcid.org/0000-0002-2652-4684; Email: qizhang@simm.ac.cn

Xuefeng Mei – School of Pharmacy, Jiangxi Medical College, Nanchang University, Nanchang 330006, People’s Republic of China²; Pharmaceutical Analytical&Solid-State Chemistry ResearchCenter, Shanghai Institute of Materia Medica, ChineseAcademy of Sciences, Shanghai 201203, People’s Republic of China; School of Chinese Materia Medica, Nanjing University of Chinese Medicine, Nan-jing 210023, People’s Republic of China; orcid.org/0000-0002-8945-5794; Email: xuefengmei@simm.ac.cn

Authors

Chenxuan Zheng – School of Pharmacy, Jiangxi Medical College, Nanchang University, Nanchang 330006, People’s Republic of China²; Pharmaceutical Analytical&Solid-State Chemistry ResearchCenter, Shanghai Institute of Materia Medica, ChineseAcademy of Sciences, Shanghai 201203, People’s Republic of China

Hao Wang – School of Chinese Materia Medica, Nanjing University of Chinese Medicine, Nan-jing 210023, People’s Republic of China

Ziyao Xiao – School of Chinese Materia Medica, Nanjing University of Chinese Medicine, Nan-jing 210023, People’s Republic of China

Zhixiong Sun – School of Pharmacy, Jiangxi Medical College, Nanchang University, Nanchang 330006, People’s Republic of China²; Pharmaceutical Analytical&Solid-State

Chemistry ResearchCenter, Shanghai Institute of Materia Medica, ChineseAcademy of Sciences, Shanghai 201203, People’s Republic of China

Junjie Bao – Pharmaceutical Analytical&Solid-State Chemistry ResearchCenter, Shanghai Institute of Materia Medica, ChineseAcademy of Sciences, Shanghai 201203, People’s Republic of China

Wenjuan Dai – Pharmaceutical Analytical&Solid-State Chemistry ResearchCenter, Shanghai Institute of Materia Medica, ChineseAcademy of Sciences, Shanghai 201203, People’s Republic of China

Complete contact information is available at:

<https://pubs.acs.org/10.1021/acsomega.4c03864>

Author Contributions

Investigation and writing—original draft preparation, C.Z.; investigation, H.W., Z.X., and Z.S.; analysis, J.B. and W.D.; Conceptualization, validation, and writing—review and editing, Q.Z.; writing—review and editing, and supervision, X.M. All authors have read and agreed to the published version of the manuscript.

Funding

This research work was financially supported by the Natural Science Foundation of Shanghai (grant no. 22ZR147390).

Notes

The authors declare no competing financial interest.

■ REFERENCES

- (1) Kijlstra, A.; Tian, Y.; Kelly, E. R.; Berendschot, T. Lutein: More than just a filter for blue light. *Prog. Retin. Eye Res.* **2012**, *31*, 303–315.
- (2) Roberts, J. E.; Dennison, J. The Photobiology of Lutein and Zeaxanthin in the Eye. *J. Ophthalmol.* **2015**, *2015*, 1–8.
- (3) Cota, F.; Costa, S.; Giannantonio, C.; Purcaro, V.; Catenazzi, P.; Vento, G. Lutein supplementation and retinopathy of prematurity: a meta-analysis. *J. Matern. Fetal Neonatal Med.* **2022**, *35*, 175–180.
- (4) Tan, J. S. L.; Wang, J. J.; Flood, V.; Rochtchina, E.; Smith, W.; Mitchell, P. Dietary antioxidants and the long-term incidence of age-related macular degeneration - The Blue Mountains Eye Study. *Ophthalmology.* **2008**, *115*, 334–341.
- (5) Mrowicka, M.; Mrowicki, J.; Kucharska, E.; Majsterek, I. Lutein and Zeaxanthin and Their Roles in Age-Related Macular Degeneration-Neurodegenerative Disease. *Nutrients* **2022**, *14*, 827.
- (6) Grether-Beck, S.; Marini, A.; Jaenicke, T.; Stahl, W.; Krutmann, J. Molecular evidence that oral supplementation with lycopene or lutein protects human skin against ultraviolet radiation: results from a double-blinded, placebo-controlled, crossover study. *Br. J. Dermatol.* **2017**, *176*, 1231–1240.
- (7) Chen, Y. M.; Wang, L.; Huang, S. X.; Ke, J. F.; Wang, Q.; Zhou, Z. W.; Chang, W. Lutein attenuates angiotensin II- induced cardiac remodeling by inhibiting AP-1/IL-11 signaling. *Redox. Biol.* **2021**, *44*, 102020.
- (8) Boon, C. S.; McClements, D. J.; Weiss, J.; Decker, E. A. Factors Influencing the Chemical Stability of Carotenoids in Foods. *Crit. Rev. Food. Sci.* **2010**, *50*, 515–532.
- (9) Ochoa Becerra, M.; Mojica Contreras, L.; Hsieh Lo, M.; Mateos Diaz, J.; Castillo Herrera, G. Lutein as a functional food ingredient: Stability and bioavailability. *J. Funct. Foods.* **2020**, *66*, 103771.
- (10) Ochoa Becerra, M.; Mojica Contreras, L.; Hsieh Lo, M.; Mateos Diaz, J.; Castillo Herrera, G. Lutein as a functional food ingredient: Stability and bioavailability. *J. Funct. Foods.* **2020**, *66*, 103771.
- (11) Arnal, E.; Miranda, M.; Johnsen-Soriano, S.; Alvarez-Nölting, R.; Díaz-Llopis, M.; Araiz, J.; Cervera, E.; Bosch-Morell, F.; Romero, F. J. Beneficial Effect of Docosahexanoic Acid and Lutein on Retinal

Structural, Metabolic, and Functional Abnormalities in Diabetic Rats. *Curr. Eye Res.* **2009**, *34*, 928–938.

(12) Xu, D. X.; Aihemaiti, Z.; Cao, Y. P.; Teng, C.; Li, X. T. Physicochemical stability, microrheological properties and microstructure of lutein emulsions stabilized by multilayer membranes consisting of whey protein isolate, flaxseed gum and chitosan. *Food Chem.* **2016**, *202*, 156–164.

(13) Zhao, C. D.; Cheng, H.; Jiang, P. F.; Yao, Y. J.; Han, J. Preparation of lutein-loaded particles for improving solubility and stability by Polyvinylpyrrolidone (PVP) as an emulsion-stabilizer. *Food Chem.* **2014**, *156*, 123–128.

(14) Tan, X. J.; Li, H. M.; Huang, W. J.; Ma, W. W.; Lu, Y. Y.; Yan, R. Enzymatic acylation improves the stability and bioactivity of lutein: Protective effects of acylated lutein derivatives on L-O2 cells upon H2O2-induced oxidative stress. *Food Chem.* **2023**, *410*, 135393.

(15) Metlicar, V.; Kranjc, K.; Albrecht, A. Utilization of Plant-Based Wastes for a Sustainable Preparation of Xanthophyll Esters via Acid Anhydrides Using β -Pinene as a Bio-Derived Solvent. *ACS Sustain. Chem. Eng.* **2021**, *9*, 10651–10661.

(16) Chitchumroonchokchai, C.; Schwartz, S. J.; Failla, M. L. Assessment of lutein bioavailability from meals and a supplement using simulated digestion and Caco-2 human intestinal cells. *J. Nutr.* **2004**, *134*, 2280–2286.

(17) Qy, X. Y.; Zeng, Z. P.; Jiang, J. G. Preparation of lutein microencapsulation by complex coacervation method and its physicochemical properties and stability. *Food Hydrocolloid.* **2011**, *25*, 1596–1603.

(18) Ding, Z.; Wang, X.; Wang, L. L.; Zhao, Y. N.; Liu, M.; Liu, W. L.; Han, J.; Prakash, S.; Wang, Z. P. Characterisation of spray dried microencapsules with amorphous lutein nanoparticles: Enhancement of processability, dissolution rate, and storage stability. *Food Chem.* **2022**, *383*, 132200.

(19) Guo, W.; Du, S. C.; Xu, S. J.; Wang, Y.; Jia, L. N.; Liu, S. Y.; Wu, S. G.; Gong, J. B.; Wang, J. K. Unraveling the Molecular Mechanisms That Influence the Color and Stability of Four Lutein Crystal Forms. *Cryst. Growth Des.* **2021**, *21*, 1762–1777.

(20) Aliasl Khiabani, A.; Tabibiazar, M.; Roufegarinejad, L.; Hamishehkar, H.; Alizadeh, A. Preparation and characterization of carnauba wax/adipic acid Oleogel: A new reinforced Oleogel for application in cake and beef burger. *Food Chem.* **2020**, *333*, 127446.

(21) Kennedy, G. L. Toxicity of adipic acid. *Drug Chem. Toxicol.* **2002**, *25*, 191–202.

(22) Jain, S.; Patel, N.; Lin, S. Solubility and dissolution enhancement strategies: current understanding and recent trends. *Drug Dev. Ind. Pharm.* **2015**, *41*, 875–887.

(23) Jarray, A.; Wijshoff, H.; Luiken, J. A.; den Otter, W. K. Systematic approach for wettability prediction using molecular dynamics simulations. *Soft Matter.* **2020**, *16*, 4299.